Journal of Alloys and Compounds 513 (2012) 455–459

Contents lists available at SciVerse ScienceDirect

Journal of Alloys and Compounds

journal homepage: www.elsevier.com/locate/jallcom

Preparation, characterization and microwave absorbing properties of FeNi alloy prepared by gas atomization method

Yongbao Feng*, Tai Qiu

College of Materials Science and Engineering, Nanjing University of Technology, No. 5 Xinmofan Road, Nanjing 210009, China

ARTICLE INFO

Article history:
Received 31 August 2011
Received in revised form 19 October 2011
Accepted 21 October 2011
Available online 7 November 2011

Keywords:
FeNi alloy
Permeability
Permittivity
Microwave absorbing material
Reflection loss

ABSTRACT

In this work, Fe–50 wt%Ni alloy was synthesized by nitrogen gas atomization method. The phase composition, morphology, element composition and saturation magnetization of the alloys were investigated by means of X-ray diffraction (XRD), scanning electron microscopy (SEM), X-ray fluorescence spectrometer (XRF) and vibrating sample magnetometer (VSM). The electromagnetic parameters and microwave absorbing properties of the microwave absorbing material made from silicone rubber and the as-prepared FeNi alloy were also studied using vector network analyzer (VNA) and transmission line theory. The results show that the particle size of most of the particles is less than 150 μm, and the average particle size is about 48 μm. The Fe–50 wt%Ni powder has a spherical shape, and the main phase composition is FCC (Fe, Ni) alloy. The as-atomized FeNi alloy possesses low coercivity and high specific saturation magnetization. As the frequency increases, the real part of relative permittivity and relative permeability of the Fe–50 wt%Ni/silicone rubber absorber decrease, while the imaginary part of relative permittivity increases. The Fe–50 wt% Ni alloy/silicone rubber absorbers with 0.8–4 mm thickness exhibit adjustable microwave absorbing properties in the range of 1–18 GHz.

1. Introduction

In recent years, microwave absorbing materials (MAMs) have been the subject of scientific interest because of their attractive abilities to reduce and eliminate the electromagnetic radiation (EMR) and electromagnetic interference (EMI) resulting from the broad applications of various kinds of electronic and microwave instruments in the gigahertz (GHz) range [1–3]. Research and design of MAMs have become essential for effective elimination of EMR and EMI in the given range of frequencies. Typically, MAMs are usually composite materials with dielectric, conductive, and/or magnetic particles embedded in a polymer matrix [4,5]. The efficiency of MAMs depends on many factors, such as conductivity, complex permittivity ($\varepsilon_r = \varepsilon' - j\varepsilon''$) and complex permeability ($\mu_r = \mu' - j\mu''$). The complex permittivity and permeability especially play an important role in the electromagnetic wave absorbing properties of the microwave absorber because the ε' and μ' determine the storage of the electromagnetic energy, and the ε'' and μ'' determine the loss of the energy [6,7]. In order to realize the maximum of the attenuation to the incident electromagnetic wave on the absorber, both the magnetic loss ($\tan\delta_\mu = \mu''/\mu'$) and dielectric loss ($\tan\delta_\varepsilon = \varepsilon''/\varepsilon'$) should be maximized [8]. According to current studies, the MAMs containing magnetic materials possess both $\tan\delta_\varepsilon$ and $\tan\delta_\mu$, which could yield large magnetic loss and dielectric loss to attenuate the electromagnetic wave [9]. As a result, many polymer composite absorbers filled with ferrite, soft magnetic metal and alloy, such as spinel ferrite [10], W type hexagonal ferrite [11], M type ferrite [12], carbonyl iron [13], FeSi [14], FeSiCr [15], and FeSiAl [16], have attracted a lot attention.

Some studies also suggested that a high permeability is favorable for improving the microwave absorbing properties, reducing the thickness and broadening the frequency bandwidth of low reflection loss (RL) [17]. However, the permeabilities of both the spinel and hexagonal ferrite will decrease sharply with increasing frequency over the GHz range due to the Snoek's limit [18], which would lead to poor performances including higher reflection loss and thicker thickness. Comparing to the conventional ferrite absorbers, the metallic soft magnetic materials can overcome the problems of the ferrite absorbers, and may be more suitable as the microwave absorbers because they possess a higher saturation magnetization and permeability that can still have a large value in a wide GHz range, which results from their higher Snoek's limits [19]. Among the metallic soft magnetic materials, FeNi alloys show excellent soft magnetic properties, and have been widely applied in the field of electronic devices and industry [20,21]. In view of their high microwave permeabilities, the microwave absorbing properties of the polymer composite absorbers filled with FeNi alloys may be immensely prominent, which have already been partly

* Corresponding author. Tel.: +86 25 83587262.
E-mail address: fyb_njut@163.com (Y. Feng).

0925-8388/$ – see front matter © 2011 Elsevier B.V. All rights reserved.
doi:10.1016/j.jallcom.2011.10.079

confirmed by some works [22–24]. Several methods have been proposed to prepare the FeNi alloys, such as solution phase route [25], hydrogen thermal reduction method [26], mechanical alloying route [27] and atomization method [28]. Many of the methods can only produce the alloys on a small scale, but the atomization technique is widely used to manufacture ultrafine metal powder and can be applied for mass production at low cost.

In this work, the Fe–50 wt%Ni alloy was synthesized via gas atomization route, and composite absorbers were prepared by using silicone rubber as the matrix and the FeNi alloys as the filler. The structures of the as-prepared FeNi alloys were characterized by SEM and XRD. The electromagnetic parameters and microwave absorbing properties of the composite absorbers were also investigated. Fe–50 wt% Ni alloy/silicone rubber absorbers with 0.8–4 mm thickness exhibited adjustable reflection loss in the range of 1–18 GHz.

2. Experimental

2.1. Powder synthesis

A master alloy with the chemical composition of Fe–50 wt%Ni was melted from the mixture of pure element Fe (99.9 wt% purity) and Ni (99.9 wt% purity) by high frequency induction melting under an argon atmosphere. In order to decrease the amount of oxygen and obtain the uniform component, the melting chamber was evacuated twice by rotary pump and backfilled with the argon in the interval, and then the master alloy was melted three times. The bulk alloy was remelted in the atomization system to a superheat temperature of 1950 K, and then atomized using a close-coupled discrete jet gas atomization nozzle at a nitrogen gas pressure of 2.0 MPa. The purpose of using the N_2 gas was to increase the cooling rate and prevent oxidation of the alloy powder. Full details of the atomization process have been reported earlier [29].

2.2. Preparation of silicone rubber absorbers

The as-prepared Fe–50 wt%Ni alloy, silicone rubber and sulfurizing agent were uniformly mixed in a rubber mixing mill for 20 min. The volume fraction of the alloy in the composite was 48%. Samples for electromagnetic parameters, which have a toroidal shape with an outer diameter of 7.0 mm and an inner diameter of 3.04 mm, were prepared by vulcanizing the mixture at 165 °C for 15 min.

2.3. Characterization

The phase constituent of the Fe–50 wt%Ni particles was characterized by X-ray diffractions (ARL X'TRA) using Cu-Kα radiation (λ = 0.1542 nm). Scanning electron microscopy (JEOL JSM 5900) and X-ray fluorescence spectrometer (ARL ADVANT'XP) were used to investigate the microstructure and the element content of the as-atomized powder. The saturation magnetization of the FeNi alloy was measured by the vibrating sample magnetometer (ADE EV5). The complex permeability and permittivity of the silicone rubber absorbers were determined using a HP 8722ET vector network analyzer and APC-7 mm coaxial line in the frequency range of 1–18 GHz.

3. Results and discussion

3.1. Particle size distribution and morphology

The atomized Fe–50 wt%Ni alloy powder was sieved according to the standard ASTM sieves in 9 size fractions, from the "under 25 μm" to the "over 150 μm". The size distribution of the FeNi alloy particles prepared by gas atomization with N_2 is listed in Table 1, and the dependence of cumulative mass distribution is shown in Fig. 1. It is shown that more than 80% of the particles are below 75 μm, and the percentage of the fine particles with the diameter of less than 25 μm is around 20%. The average particle size (d_{50}) is about 48 μm.

The SEM images of the FeNi particles are shown in Fig. 2. From the general landscape of Fig. 2a, it can be observed that numerous particles have a small diameter, and some coarse particles also can be found. The distribution of particle size is consistent with the mass fraction. Most of the particles have the spherical form; however, there are still a few particles with nonspherical shape, which may be formed by a large particle being caped with small ones.

Table 1
Particle size distribution of the gas atomized Fe–50 wt%Ni powders.

Particle size (μm)	Mass fraction (%)
<25	19.72
25–38	15.23
38–48	15.12
48–58	14.98
58–75	15.79
75–106	9.74
106–115	6.31
115–150	2.61
>150	0.50

Previous studies with similar results have been reported, and the reasons may be explained as follows [30]: (1) the large droplets may still be in a liquid or semi-solid state while the smaller ones have been already solidified. The particles with different diameter have the different solidification rate (SR), which results in the higher SR of smaller particles and the lower SR of larger ones; (2) the larger droplets will readily solidified. Therefore, these particles with different states will adhere together easily during the collision in the jet gas turbulence. From Fig. 2b, it is also found that the surface of the particle is relatively smooth.

It should be noted that the FeNi alloy has a wide size distribution. The electromagnetic absorbing agents are usually filled in the polymer, and a higher bulk density is helpful to improve the filling factor. The wide particle size distribution of the Fe–50 wt%Ni prepared in this work will increase the packing density, which might lead to the higher volume fraction in the silicone rubber absorber.

3.2. Elementary analysis, X-ray diffraction and hysteresis loop

In order to find whether the elemental composition of the Fe–50 wt%Ni is the same as what it was designed and weighed to be, the chemical composition of the as-prepared FeNi alloy was analyzed using XRF. The result shows that the ratio between Fe and Ni is 49.89:49.92, and the rest of the composition including Si, Al and Cu are 0.11. According to the analysis, it can be reasoned that the balance should be oxygen, which means the Fe–50 wt%Ni may be slightly oxidized.

The XRD analysis was conducted to determine the phase composition of the atomized FeNi alloy particles, which is shown in Fig. 3. From the XRD pattern, only three diffraction peaks can be found in the range of 10–80°. The peaks for the Fe–50 wt%Ni alloy appear to be strong, which are attributed to the FCC (Fe, Ni) alloy called taenite phase with space group F*m*3*m* according to the JCPDS card number 47-1417. This confirms that the smelting process of the master alloy is perfectly right and sensible. The finding is consistent with the previous studies in which mechanical alloying method was employed to prepare the FeNi alloys [31].

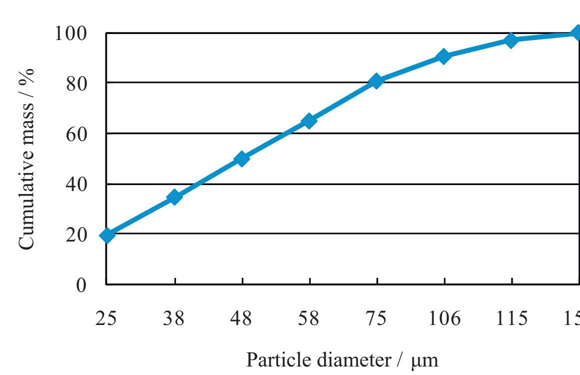

Fig. 1. Dependence of cumulative mass distribution on the particle size.

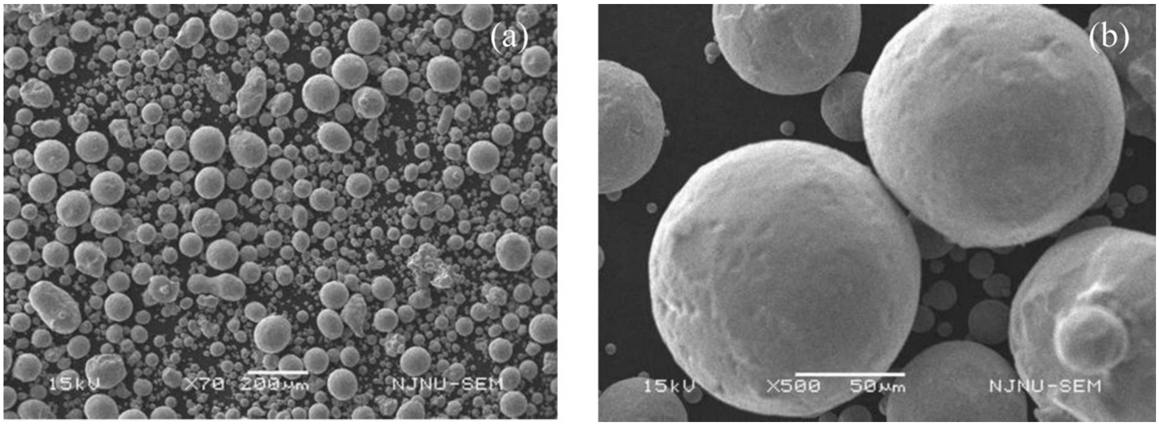

Fig. 2. SEM images of the atomized Fe–50 wt%Ni powder.

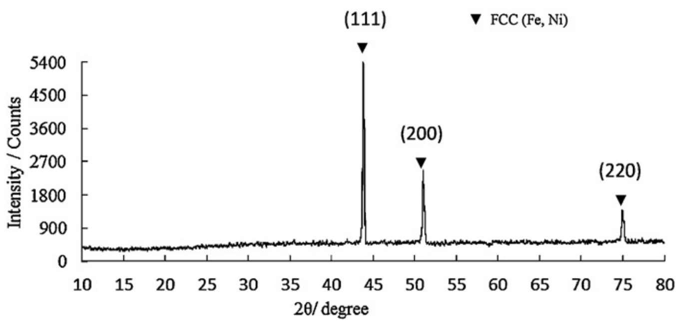

Fig. 3. XRD pattern of the atomized FeNi alloy.

Fig. 4 shows the field dependence of hysteresis loop for the as-atomized FeNi alloy. It can be seen that the Fe–50 wt%Ni possesses the low coercivity H_c and high specific saturation magnetization σ_s, which were about 3.83 Oe and 165 emu/g, respectively. The H_c is lower and the σ_s is higher than the values reported by Guittoum et al. [32]. The relationship between the permeability and saturation magnetization can be expressed as follows [33]:

$$\mu_i = 1 + \frac{(4\pi M_s)^2}{(4\pi M_s)H_a - (f/2.8)^2 + j\alpha(4\pi M_s)(f/2.8)} \tag{1}$$

where f is the frequency, M_s is the saturation magnetization and H_a is the magnetic anisotropy field.

From the above equation, it is clear that that μ_i increases with the increasing of M_s and the decreasing of H_a. Based on the magnetic theory, the Fe–50 wt%Ni alloy must have the higher M_s and lower H_a due to the high σ_s, low H_c and spherical shape, which are favorable to improve the permeability. As is commonly known, higher permeability can enlarge the absorption bandwidth and decrease the reflection loss, therefore, microwave absorbing material filled with the as-prepared FeNi alloy may possess excellent electromagnetic parameters and microwave absorbing properties.

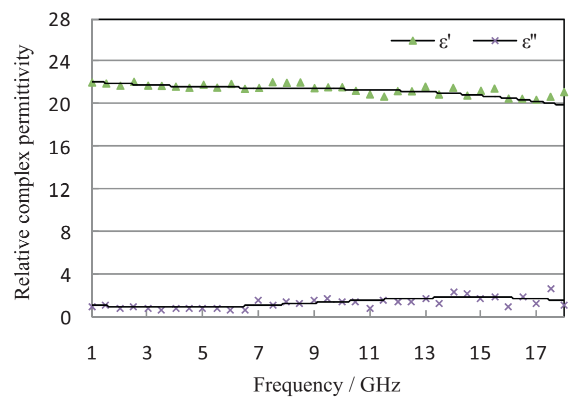

Fig. 5. Frequency dependence of complex permittivity for the Fe–50 wt%Ni/silicone rubber absorber.

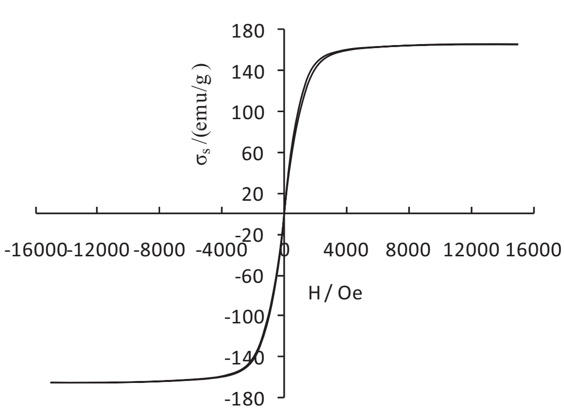

Fig. 4. Hysteresis loop of the atomized FeNi alloy.

3.3. Electromagnetic parameters and reflection loss

The relative complex permittivity and permeability of the Fe–50 wt%Ni alloy/silicone rubber composite absorber were investigated, and the results are shown in Figs. 5 and 6, which illustrate

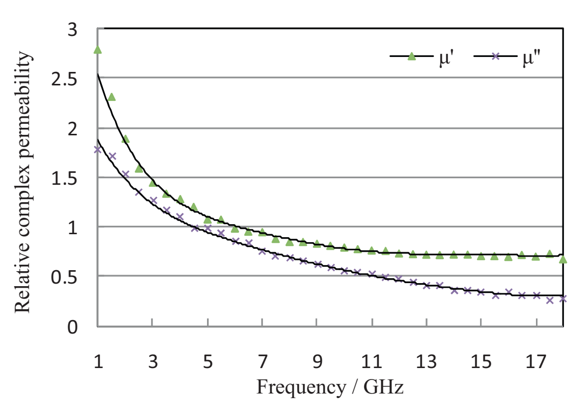

Fig. 6. Frequency dependence of complex permeability for the Fe–50 wt%Ni/silicone rubber absorber.

Table 2
Microwave absorbing properties of the silicone absorbers with the thickness of 0.8–1.5 mm.

Thickness (mm)	0.8	0.9	1.0	1.1	1.2	1.3	1.4	1.5
Minimum RL (dB)	−4.6	−7.1	−10.3	−10.7	−9.9	−9.0	−8.5	−8.4
Frequency of the minimum RL (GHz)	18.0	18.0	18.0	17.1	16.0	13.7	11.9	11.0
Bandwidth of RL <−8 dB (GHz)	\	\	1.49	3.08	3.80	3.38	2.64	1.79

Table 3
Microwave absorbing properties of the silicone absorbers with the thickness of 1.5–4.0 mm.

Thickness (mm)	1.5	2.0	2.5	3.0	3.5	4.0
Minimum RL (dB)	−8.4	−8.7	−9.5	−10.9	−11.5	−12.2
Frequency of the minimum RL (GHz)	11.0	7.2	5.1	3.8	3.0	2.8
Bandwidth of RL <−8 dB (GHz)	1.79	1.83	2.16	1.83	1.79	1.73

the permittivity and permeability as a function of the frequency in the range of 1–18 GHz.

Fig. 5 shows that the real part ε' of relative complex permittivity decreases a little bit with the increase of the frequency, and it ranges from 20.37 to 22.02. However, the imaginary part ε'' of relative complex permittivity increases as the frequency increases. It is well known that the interfacial polarization can be induced at lower frequency, and will not keep up with the change of the alternating electric field as the frequency increases [34]. Moreover, in the high frequency range, the dielectric loss is determined by electric conductance loss and relaxation polarization loss that increases as the frequency increases [35]. Thus, it is reasonable that the ε' decreases while the ε'' increases with the increasing of frequency.

From Fig. 6, it can be found that the real part μ' and imaginary part μ'' of complex permeability of the silicone rubber composite absorber filled with Fe–50 wt%Ni present the different variations from the frequency spectra of complex permittivity, and both the μ' and μ'' gradually decrease as the frequency increases. The decrease of permeability may be due to the hysteresis of domain-wall motion and rotation as the frequency increases, which has been found by many researchers [2].

According to the transmission line theory, the reflection loss (RL) can be calculated from the relative complex permittivity and permeability at a given frequency and the thickness of the microwave absorbing material. The RL under normal incidence of the electromagnetic field on the surface of a single-layer absorber backed with a perfect conductor can be defined as follows [17]:

$$RL\ (\text{dB}) = 20\log\left|\frac{Z_{in}-Z_0}{Z_{in}+Z_0}\right| \tag{2}$$

Here, Z_0 is the impedance of air, and Z_{in} is the input impedance of the absorber, which were given by:

$$Z_0 = \sqrt{\frac{\mu_0}{\varepsilon_0}} \tag{3}$$

$$Z_{in} = \sqrt{\frac{\mu_r\mu_0}{\varepsilon_r\varepsilon_0}}\tanh\left[j\left(\frac{2\pi fd}{c}\right)\sqrt{\mu_r\mu_0\varepsilon_r\varepsilon_0}\right] \tag{4}$$

where ε_0 and μ_0 are the permittivity and permeability of vacuum, ε_r and μ_r are the relative complex permittivity and permeability, respectively of the composite absorber, f is the frequency, d is the thickness of the absorber and c is the velocity of light in free space.

Fig. 7 shows the frequency dependences of the calculated reflection losses of the Fe–50 wt%Ni/silicone rubber absorbers with thickness of 0.8–4.0 mm, and the detailed microwave absorbing properties including minimum RL, frequency of the minimum RL and bandwidth of RL < −8 dB are provided in Tables 2 and 3. It can be found that the thickness of the silicone absorber has an important influence on the microwave absorbing properties. There is no peak to be found in the curves of reflection loss, and the minimum reflection loss decreases with the increase of thickness when the thickness is less than 1.1 mm. However, the variation curves of the reflection loss present the single apex types when the thickness is in the range of 1.1–3.0 mm, and double apex curves can be observed in higher frequencies when the thickness is more than 3.0 mm. When the thickness is greater than 1.1 mm, the minimum RL increases at first and then decreases as the thickness increases. The peak frequency of the reflection loss shifts toward the low frequency band. The thickness of 1.5 mm seems to be crucial for the microwave absorbing properties of the Fe–50 wt%Ni/silicone rubber absorber. The absorption peak of the absorbers with a thickness less than 1.5 mm is in the high frequency, and on the contrary, the absorption peak of the absorbers with the thickness greater than 1.5 mm will be in the low frequency. In other words, the thin Fe–50 wt%Ni/silicone rubber absorbers possess low RL in high frequency, and the thick absorber has distinguished properties in low frequency.

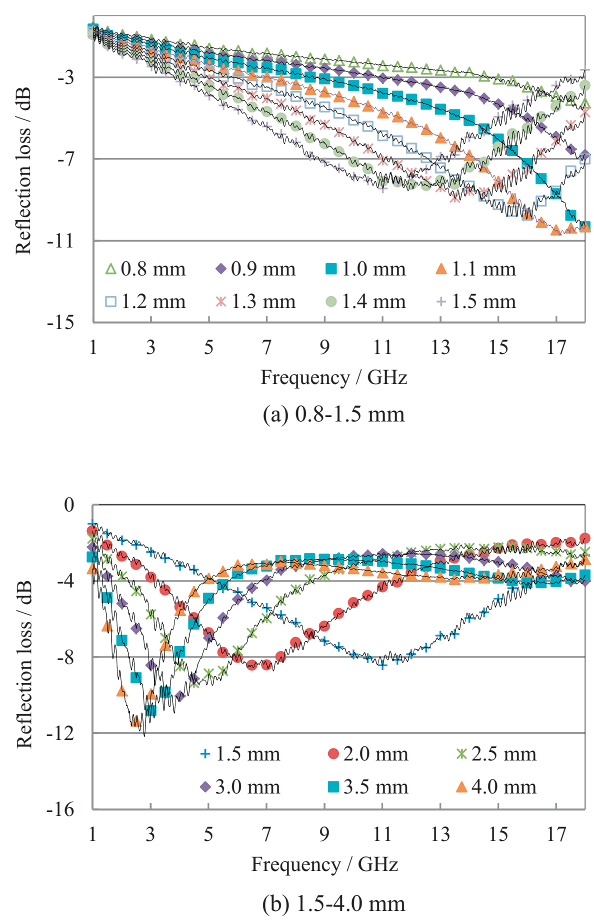

Fig. 7. The frequency dependences of the calculated reflection losses of the Fe–50 wt%Ni/silicone rubber absorbers with thickness of 0.8–4.0 mm.

In consideration of both the minimum RL and the bandwidth of RL < −8 dB, the absorbers with the thickness of 1.2 mm and 2.5 mm exhibit the best microwave absorbing properties, and the minimum RLs are −9.9 dB at 16.0 GHz and −9.5 dB at 5.1 GHz; the bandwidths of RL < −8 dB are 3.8 GHz and 2.16 GHz. A previous study showed that the peak frequency of the absorber with the thickness of 2.5 mm was around 11 GHz [26], which is significantly different from our results. However, the effects of the thickness on the microwave absorbing properties are similar to what has been previously reported. The minimum reflections can be obtained at given frequencies if the thickness of the absorber (t) satisfies [22]:

$$t = \frac{nc}{4f\sqrt{|\mu_r||\varepsilon_r|}} \quad (n = 1, 3, 5, \ldots) \tag{5}$$

where c is the speed of the light, f is the frequency, ε_r and μ_r are the relative complex permittivity and permeability. Eq. (5) indicates that thickness is inversely proportional to peak frequency, therefore, the peak frequency will shift toward low frequency band as the thickness increases. From Eq. (5), it is not hard to find the reason that the peak frequency of 2.5 mm absorber in our work is around 5.1 GHz, while the one in the previous study is 11 GHz. That is because the higher ε_r and μ_r obtained in this work will result in the low peak frequency under the same thickness.

4. Conclusions

In summary, spherical Fe–50 wt%Ni alloy with the phase composition of taenite was synthesized by the nitrogen gas atomization method. The as-prepared FeNi alloy exhibits excellent soft magnetic performances, and the coercivity H_c and specific saturation magnetization σ_s are 3.83 Oe and 165 emu/g. The microwave absorbing properties of Fe–50 wt%Ni/silicon rubber absorbers are seriously affected by the thickness. The thin and thick absorbers show the better performances in the high and low frequency, respectively. The absorber with thickness of 1.2 mm possesses the minimum RL of −9.9 dB at 16.0 GHz, and the bandwidth of RL < −8 dB is 3.8 GHz. The 2.5 mm absorber has the minimum RL of −9.5 dB at 5.1 GHz, and the bandwidth of RL < −8 dB is 2.16 GHz.

Acknowledgements

This work has been supported by the Natural Science Foundation of the Higher Education Institutions of Jiangsu Province (No. 09KJB430006) and Science Foundation of Nanjing University of Technology.

References

[1] H. Bayrakdar, Complex permittivity, complex permeability and microwave absorption properties of ferrite-paraffin polymer composites, J. Magn. Magn. Mater. 323 (2011) 882–1885.
[2] R.S. Meena, S. Bhattachrya, R. Chatterjee, Complex permittivity permeability and microwave absorbing studies of ($Co_{2-x}Mn_x$) U-type hexaferrite for X-band (8.2–12.4 GHz) frequencies, Mater. Sci. Eng. B: Solid State Adv. Technol. 171 (2010) 133–138.
[3] C.C. Lee, Y.Y. Cheng, H.Y. Chang, D.H. Chen, Synthesis and electromagnetic wave absorption property of Ni–Ag alloy nanoparticles, J. Alloys Compd. 480 (2009) 74–680.
[4] J.F. Xu, M.Y. Koledintseva, S. De, A. Radchenko, R.E. DuBroff, J.L. Drewniak, Y.X. He, R. Johnson, FDTD modeling of absorbing materials for EMI applications, in: Proceedings of the Asia-Pacific Symp. Electromagn. Compat., APEMC, Beijing, April 12–16, 2010, pp. 173–176.
[5] H. Zou, S.H. Li, L.Q. Zhang, S.N. Yan, H.G. Wu, S. Zhang, M. Tian, Determining factors for high performance silicone rubber microwave absorbing materials, J. Magn. Magn. Mater. 323 (2011) 643–1651.
[6] L.D. Liu, Y.P. Duan, S.H. Liu, L.Y. Chen, J.B. Guo, Microwave absorption properties of one thin sheet employing carbonyl-iron powder and chlorinated polyethylene, J. Magn. Magn. Mater. 322 (2010) 736–1740.
[7] T.H. Ting, K.H. Wu, Synthesis, characterization of polyaniline/$BaFe_{12}O_{19}$ composites with microwave-absorbing properties, J. Magn. Magn. Mater. 322 (2010) 160–2166.
[8] S.W. Phang, M. Tadokoro, J. Watanabe, N. Kuramoto, Effect of Fe_3O_4 and TiO_2 addition on the microwave absorption property of polyaniline micro/nanocomposites, Polym. Adv. Technol. 20 (2009) 550–557.
[9] X. Wang, R.Z. Gong, H. Luo, Z.K. Feng, Microwave properties of surface modified Fe–Co–Zr alloy flakes with mechanochemically synthesized polystyrene, J. Alloys Compd. 480 (2009) 61–764.
[10] F. Gao, D.L. Zhao, Z.M. Shen, Preparation and microwave absorbing properties of Cu-doped Ni–Zn spinel ferrites, Adv. Mater. Res. 105–106 (2010) 293–296.
[11] A. Oikonomou, T. Giannakopoulou, G. Litsardakis, Design, fabrication and characterization of hexagonal ferrite multi-layer microwave absorber, J. Magn. Magn. Mater. 316 (2007) 827–830.
[12] Y.J. Kim, S.S. Kim, Magnetic and microwave absorbing properties of Ti and Co substituted M-hexaferrites in Ka-band frequencies (26 540 GHz), J. Electroceram. 24 (2010) 314–318.
[13] W.P. Li, L.Q. Zhu, G. Jing, H.C. Liu, Microwave absorption properties of fabric coated absorbing material using modified carbonyl iron power, Compos. Part B: Eng. 42 (2011) 626–630.
[14] L.D. Liu, Y.P. Duan, J.B. Guo, L.Y. Chen, S.H. Liu, Influence of particle size on the electromagnetic and microwave absorption properties of FeSi/paraffin composites, Phys. B: Condens. Matter 406 (2011) 2261–2265.
[15] M.S. Kim, E.H. Min, J.G. Koh, Comparison of the effects of particle shape on thin FeSiCr electromagnetic wave absorber, J. Magn. Magn. Mater. 321 (2009) 81–585.
[16] S.J. Lee, Y.B. Kim, K.S. Lee, D.J. Byun, S.W. Kim, Effect of annealing temperature on electromagnetic absorption properties of crystalline Fe–Si–Al alloy powder–polymer composites, Phys. Stat. Sol. A: Appl. Mater. 204 (2007) 4121–4124.
[17] B.S. Zhang, Y. Feng, J. Xiong, Y. Yang, H.X. Lu, Microwave-absorbing properties of de-aggregated flake-shaped carbonyl-iron particle composites at 2–18 GHz, IEEE Trans. Magn. 42 (2006) 1778–1781.
[18] R. Sharma, R.C. Agarwala, V. Agarwala, Development of electroless (Ni–P)/$BaNi_{0.4}Ti_{0.4}Fe_{11.2}O_{19}$ nanocomposite powder for enhanced microwave absorption, J. Alloys Compd. 467 (2009) 57–365.
[19] W.F. Yang, L. Qiao, J.Q. Wei, Z.Q. Zhang, T. Wang, F.S. Li, Microwave permeability of flake-shaped FeCuNbSiB particle composite with rotational orientation, J. Appl. Phys. 107 (2010) 033913.
[20] I. Chicinas, O. Geoffroy, O. Isnard, V. Pop, AC magnetic properties of the soft magnetic composites based on nanocrystalline Ni–Fe powders obtained by mechanical alloying, J. Magn. Magn. Mater. 310 (2007) 474–2476.
[21] Y. Shirakata, N. Hidaka, M. Ishitsuka, A. Teramoto, T. Ohmi, High permeability and low loss Ni–Fe composite material for high-frequency applications, IEEE Trans. Magn. 44 (2008) 2100–2106.
[22] J.Q. Wei, Z.Q. Zhang, B.C. Wang, T. Wang, F.S. Li, Microwave reflection characteristics of surface-modified $Fe_{50}Ni_{50}$ fine particle composites, J. Appl. Phys. 108 (2010) 123908.
[23] X.G. Liu, B. Li, D.Y. Geng, W.B. Cui, F. Yang, Z.G. Xie, D.J. Kang, Z.D. Zhang, (Fe Ni)/C nanocapsules for electromagnetic-wave-absorber in the whole Ku-band, Carbon 47 (2009) 470–474.
[24] X.G. Liu, Z.Q. Ou, D.Y. Geng, Z. Han, J.J. Jiang, W. Liu, Z.D. Zhang, Influence of a graphite shell on the thermal and electromagnetic characteristics of FeNi nanoparticles, Carbon 48 (2010) 891–897.
[25] Z.Y. Zhang, X.X. Liu, Y.P. Wu, Synthesis, characterization and microwave absorption properties of $SrFe_{12}O_{19}$ ferrites and $FeNi_3$ nanoplatelets composites, Adv. Mater. Res. 148-149 (2011) 893–896.
[26] L. Zhen, Y.X. Gong, J.T. Jiang, W.Z. Shao, Electromagnetic properties of FeNi alloy nanoparticles prepared by hydrogen-thermal reduction method, J. Appl. Phys. 104 (2008) 034312.
[27] R. Koohkan, S. Sharafi, H. Shokrollahi, K. Janghorban, Preparation of nanocrystalline Fe–Ni powders by mechanical alloying used in soft magnetic composites, J. Magn. Magn. Mater. 320 (2008) 089–1094.
[28] J.E. Flinn, G.R. Smolik, Intrinsic features of Fe–40 wt.%Ni powders prepared by centrifugal or vacuum gas atomization, Mater. Sci. Eng. A: Struct. Mater. Prop. Microstruct. Process 124 (1990) 39–48.
[29] S.J. Hong, T.S. Kim, H.S. Kim, W.T. Kim, B.S. Chun, Microstructural behavior of rapidly solidified and extruded Al–14 wt%Ni–14 wt%Mm (Mm, Misch metal) alloy powders, Mater. Sci. Eng. 271 (1999) 469–476.
[30] P. Dong, W.L. Hou, X.C. Chang, M.X. Quan, J.Q. Wang, Amorphous and nanostructured $Al_{85}Ni_5Y_6Co_2Fe_2$ powder prepared by nitrogen gas-atomization, J. Alloys Compd. 436 (2007) 18–123.
[31] S.D. Kaloshkin, V.V. Tcherdyntsev, I.A. Tomilin, Yu.V. Baldokhin, E.V. Shelekhov, Phase transformations in Fe–Ni system at mechanical alloying and consequent annealing of elemental powder mixtures, Phys. B: Condens. Matter 299 (2001) 236–241.
[32] A. Guittoum, A. Layadi, A. Bourzami, H. Tafat, N. Souami, S. Boutarfaia, D. Lacour, X-ray diffraction, microstructure, Mössbauer and magnetization studies of nanostructured $Fe_{50}Ni_{50}$ alloy prepared by mechanical alloying, J. Magn. Magn. Mater. 320 (2008) 385–1392.
[33] L.Z. Wu, J. Ding, H.B. Jiang, L.F. Chen, C.K. Ong, Particle size influence to the microwave properties of iron based magnetic particulate composites, J. Magn. Magn. Mater. 285 (2005) 33–239.
[34] M.G. Han, W. Tang, W.B. Chen, H. Zhou, L.J. Deng, Effect of shape of Fe particles on their electromagnetic properties within 1–18 GHz range, J. Appl. Phys. 107 (2010) 09A958.
[35] Y.B. Feng, T. Qiu, C.Y. Shen, Absorbing properties and structural design of microwave absorbers based on carbonyl iron and barium ferrite, J. Magn. Magn. Mater. 318 (2007) 8–13.